Supplementary Information

Novel multi-carboxyl functionalized MOF platform for effective photodynamic therapy with hypoxia modulation based on prominent self-oxygen generation

Guorui Gao[a‡], Yifan Wang[a‡], Yu Jiang[a], Shiping Luo[a], Mengnan Li[a], Yanyu Cao[a], Yu Ma[a]* and Bo Tang[a,b]*

[a] College of Chemistry, Chemical Engineering and Materials Science, Collaborative Innovation Center of Functionalized Probes for Chemical Imaging in Universities of Shandong, Key Laboratory of Molecular and Nano Probes, Ministry of Education, Institute of Molecular and Nano Science, Shandong Normal University, Jinan 250014, P. R. China.

[b] Laoshan Laboratory, Qingdao, 266200, P. R. China.

Corresponding. author e-mail: may@sdnu.edu.cn; tangb@sdnu.edu.cn.

1. Materials and methods

Materials. The chemicals were obtained from commercial sources and used without further purification. Benzenetetracarboxylic acid, zirconyl chloride octahydrate, Ferric chloride hexahydrate, indocyanine gree (ICG), hydrogen peroxide (H_2O_2; 30% aqueous solution), titanium sulfate, 1,3-Diphenylisobenzofuran (DPBF), Tris(4,7-diphenyl-1,10-phenanthroline)ruthenium(II) dichloride (RDPP), 3-(4,5-dimethylthiazol-2-yl)-2,5-diphenyltetrazolium bromide (MTT), Dulbecco's modified Eagle's medium (DMEM) were purchased from Sigma-Aldrich (Shanghai, China). Fetal bovine serum (FBS) was purchased from Biological Industries. Calcein-AM/PI double staining kit, 2′,7′-Dichlorofluorescein diacetate (DCFH-DA), Annexin V-FITC Apoptosis Detection Kit were purchased from Beyotime Biotechnology (China).Ultrapure water (18.2 MΩ cm) was get from a Water Pro water purification system (Labconco Corp., Kansas City, MO). Human cervical carcinoma cells HeLa cells were purchased from the Committee on Type Culture Collection of the Chinese Academy of Sciences.

Physical Measurements. Powder X-ray (PXRD) patterns were recorded on a Bruker SMART APEX CCD-based diffractometer. Transmission electron microscopy (TEM) images were recorded on a JEM-100CX II electron microscope. Energy dispersive spectroscopy (EDS) mapping analysis was taken on a SUPRA 55 scanning electron microscope. The dynamic light scattering (DLS) experiment was carried out using a Malvern Nano-ZS90 instrument. The Fourier transform infrared (FT-IR) spectra were recorded on a Bruker ALPHA FT-IR spectrometer. Absorption spectra were recorded on a Hitachi U-4100 UV–vis spectrophotometer. The fluorescence spectra were obtained on a FLS-980 Edinburgh fluorescence spectrometer. In the MTT assay, absorbance was performed

on a microplate reader (Synergy 2, Biotek, USA). The Confocal fluorescence images were obtained by a Leica TCS SP8. Imaging flow cytometry was accomplished on Amnis ImageStream MarkII (Merck Millipore, Seattle, WA).

2. Synthesis of UMOF-c

The multi-carboxyl ligands 1,2,4,5-benzenetetracarboxylic acid (2.54 g, 10 mmol) and $ZrCl_4$ (2.43 mg, 10.4 mmol) were mixed in 60 mL of water and 40 mL of acetic acid, and then the mixture was refluxed for 24 h [1]. After being collected and washed with water, the nanoscale crystals UMOF-c were collected and washed with water several times and then dried in vacuum for 24 h.

3. Synthesis of MF-c

3 mg UMOF-c was dispersed in 5 mL of water and then 25.92 mg $FeCl_3 \cdot 6H_2O$ was added. The mixture was then stirred for 12 h at 60 °C. After being cooled to the room temperature, the product MF-c was collected by centrifugal separation and washed with water three times.

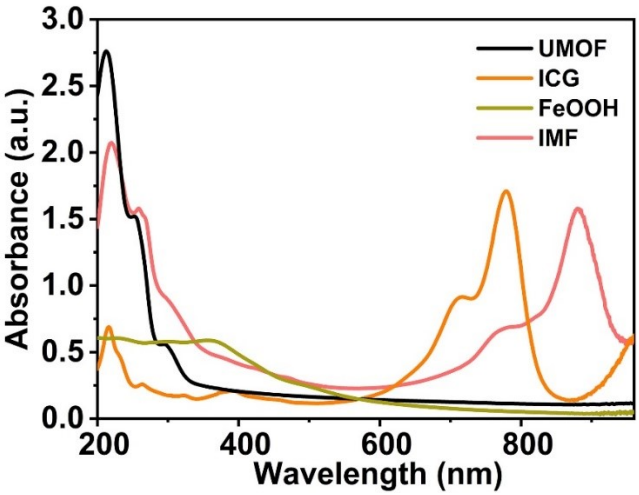

Fig. S1 UV-vis absorption spectra of UMOF, ICG, FeOOH and IMF.

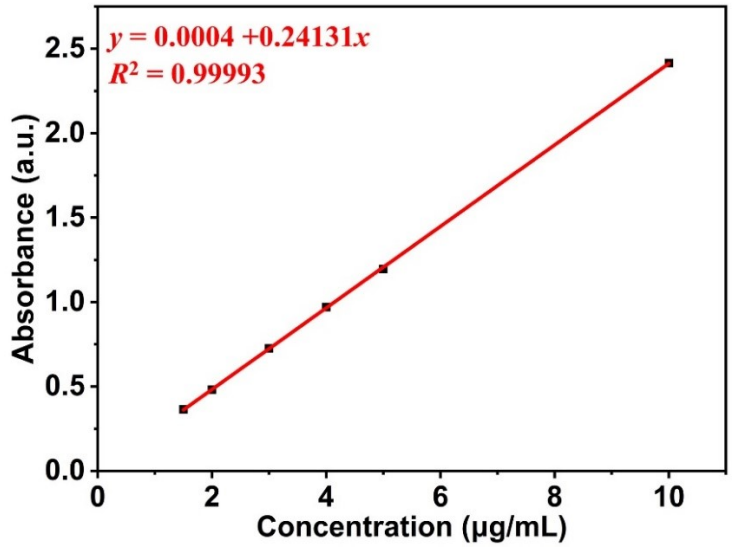

Fig. S2 Linear correlation between absorption intensity and the corresponding concentration of ICG (1.5 μg mL^{-1}, 2 μg mL^{-1}, 3 μg mL^{-1}, 4 μg mL^{-1}, 5 μg mL^{-1} and 10 μg mL^{-1}).

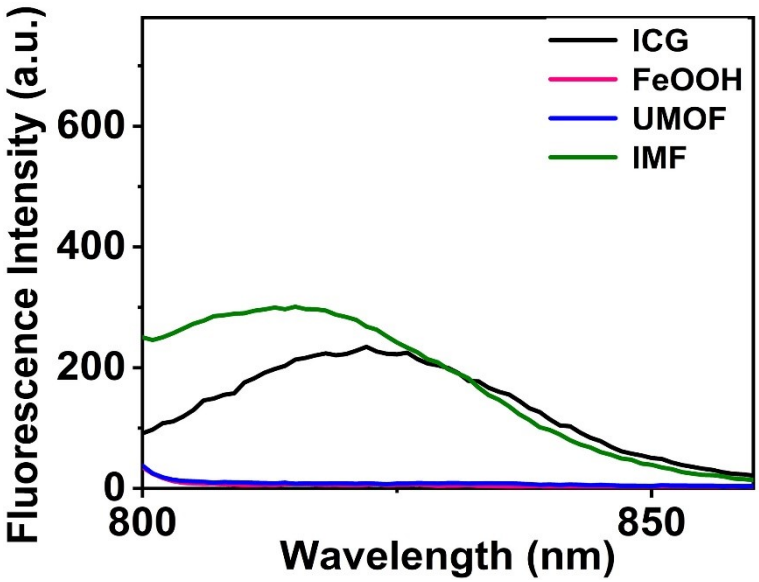

Fig. S3 Fluorescence spectra of ICG, FeOOH, UMOF and IMF.

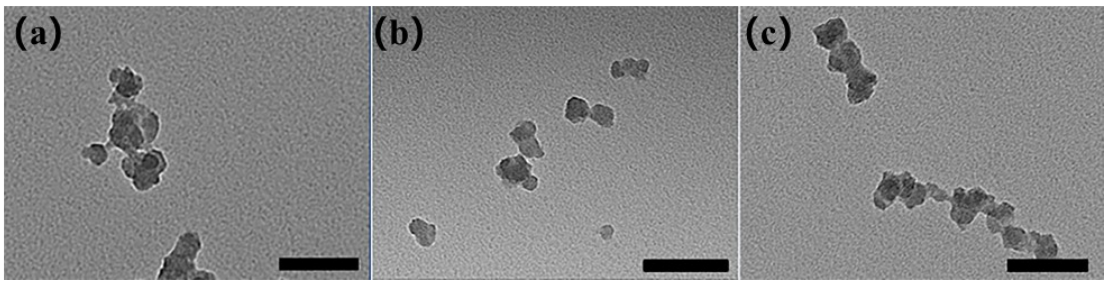

Fig. S4 TEM images of (a) UMOF, (b) MF, (c) IMF (Scale bar = 200 nm).

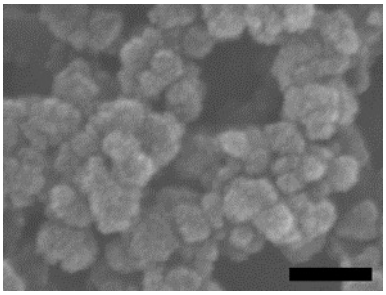

Fig. S5 SEM image of the IMF (Scale bar = 200 nm).

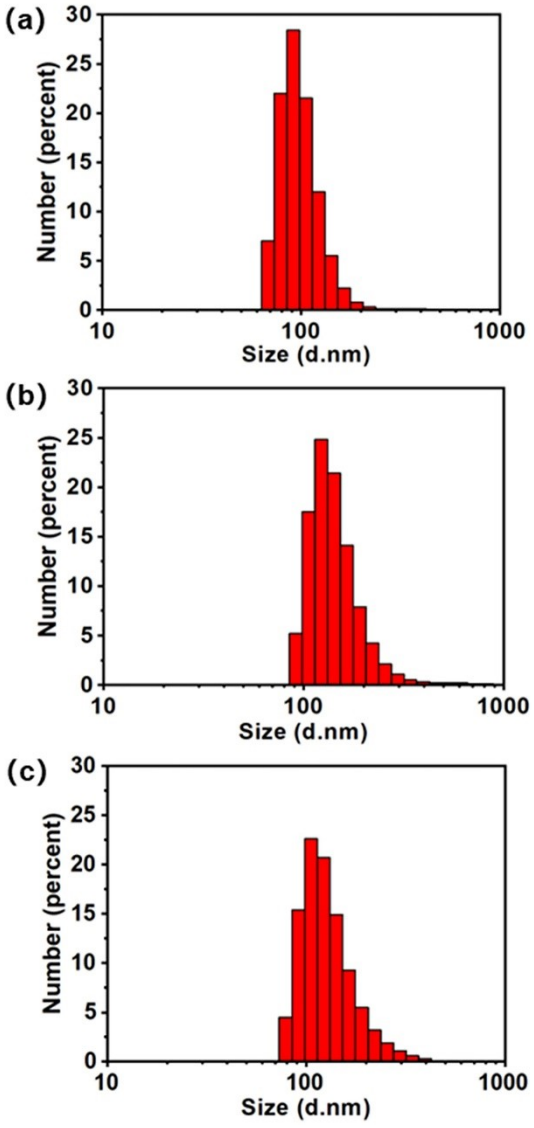

Fig. S6 DLS data of (a) UMOF, (b) MF and (c) IMF.

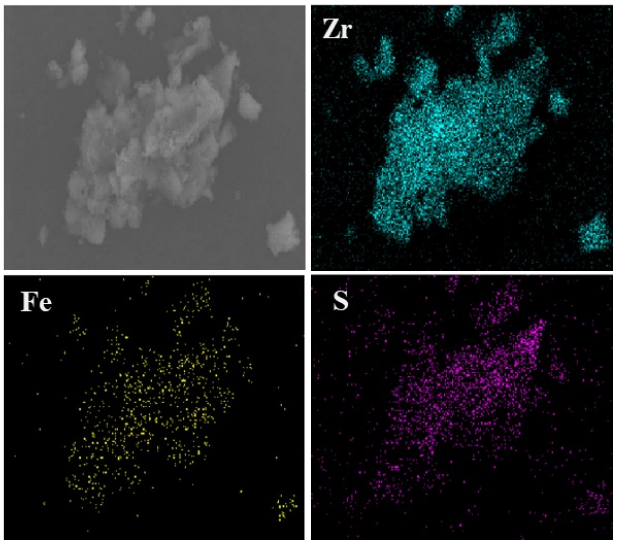

Fig. S7 SEM-mapping images of IMF.

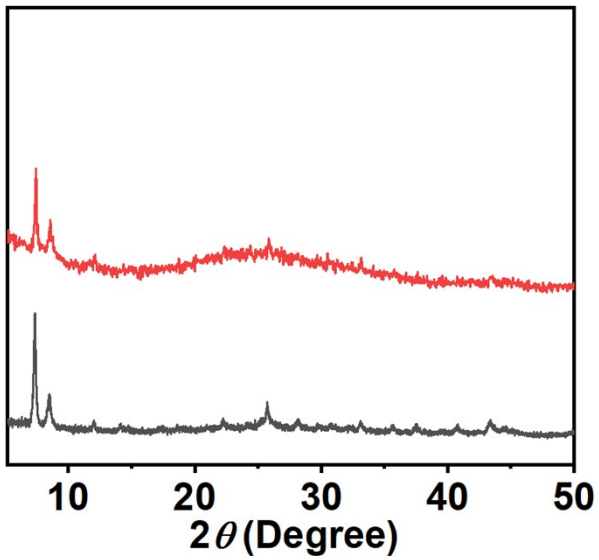

Fig. S8 PXRD patterns of UMOF-c (black line) and MF-c (red line).

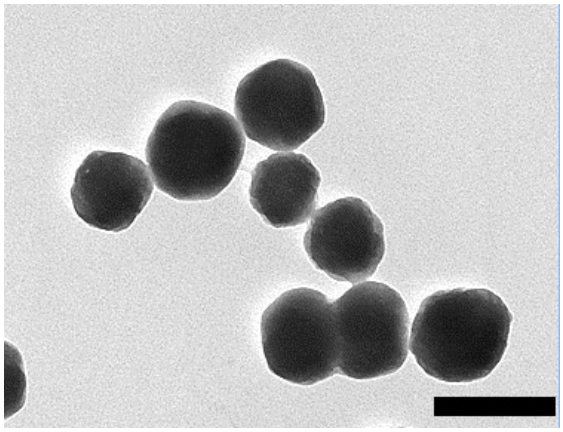

Fig. S9 TEM images of UMOF-c (Scale bar = 200 nm).

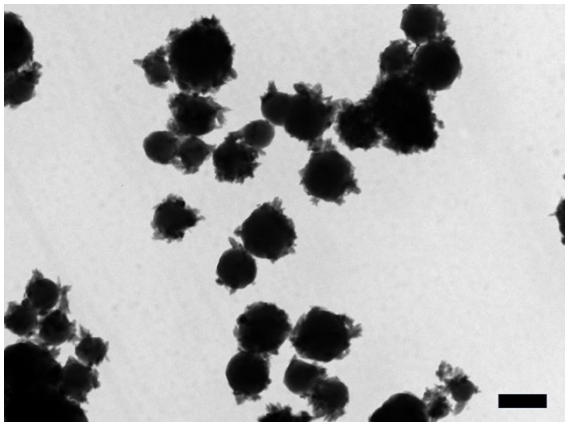

Fig. S10 TEM images of MF-c (Scale bar = 200 nm).

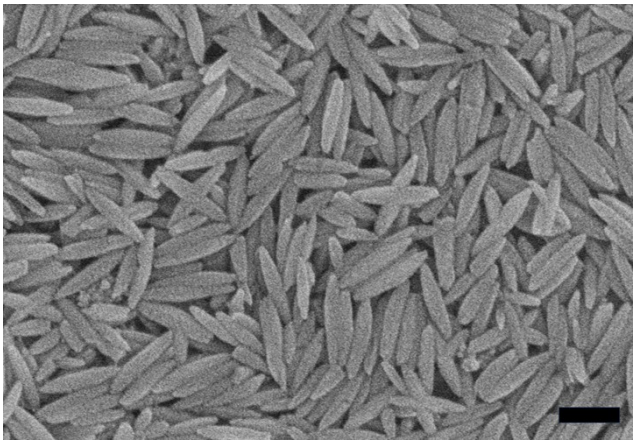

Fig. S11 SEM image of the FeOOH (Scale bar = 200 nm).

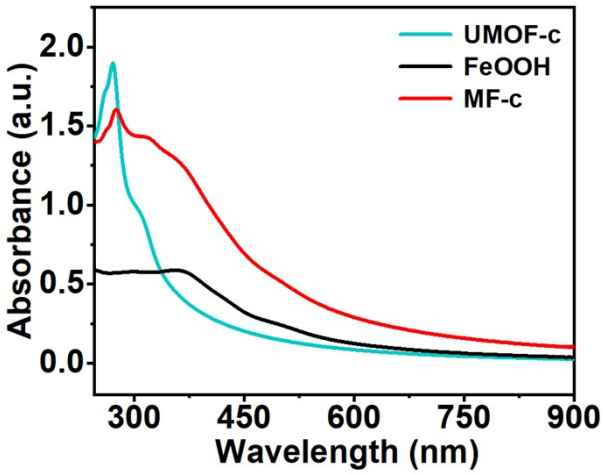

Fig. S12 UV-vis absorption spectra of UMOF-c, FeOOH and MF-c.

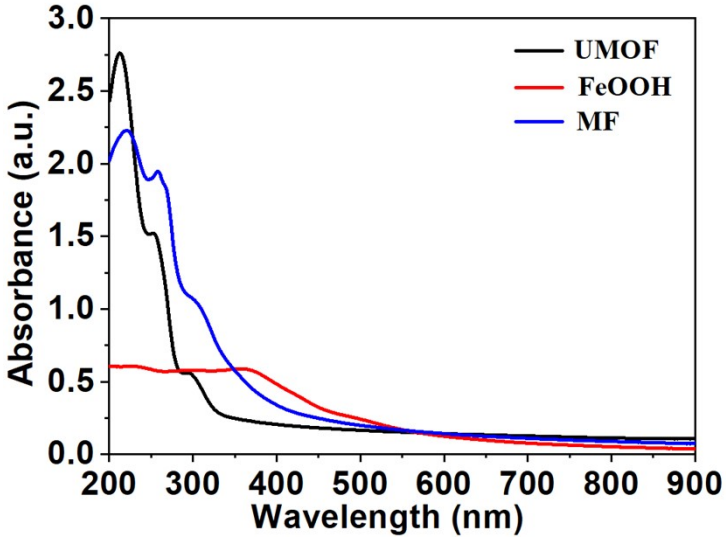

Fig. S13 UV-vis absorption spectra of UMOF, FeOOH and MF.

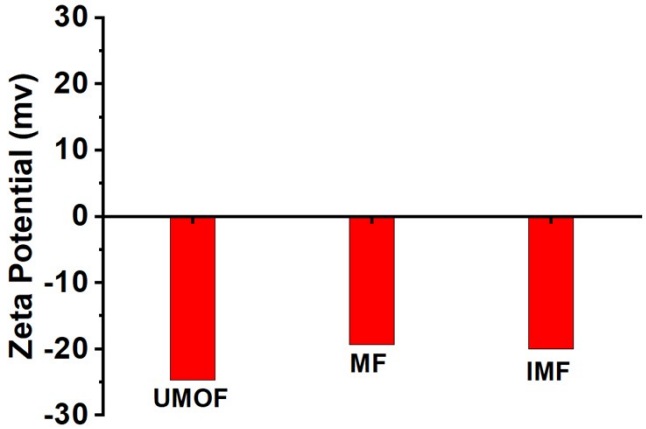

Fig. S14 Zeta potential diagram for UMOF, MF and IMF.

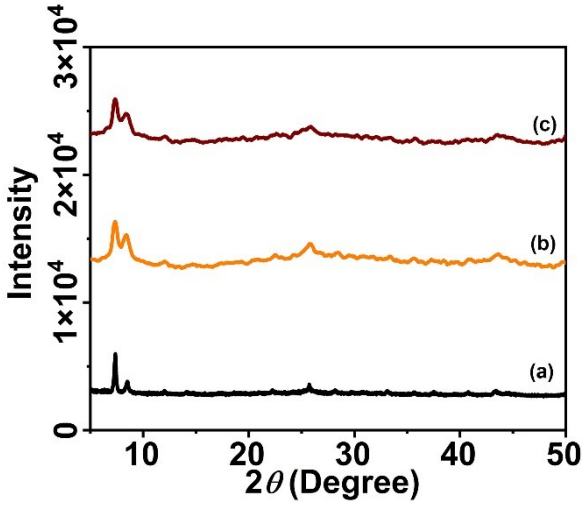

Fig. S15 PXRD patterns of (a) UiO-66, (b) IMF after being immersed in PBS buffer solution and (c) IMF after being immersed in the acetic acid/sodium acetate buffer solution for 24 hours.

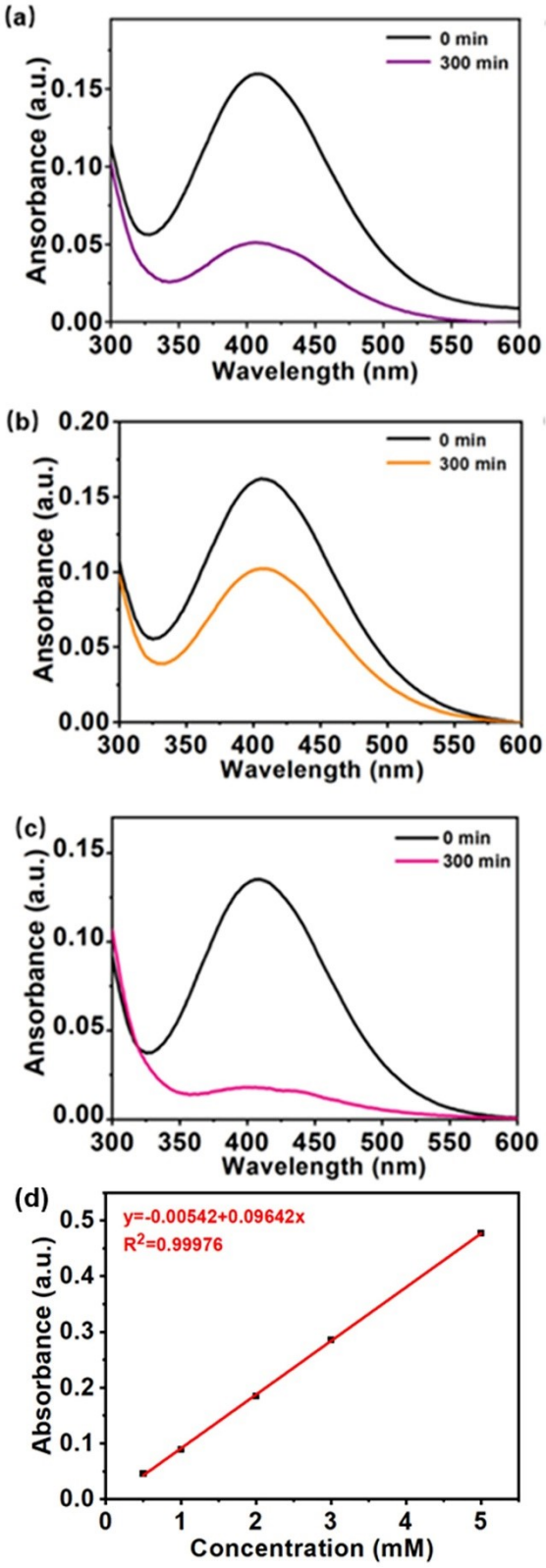

Fig. S16 UV-vis absorption spectra for IMF synthesized by different amounts of UMOF in the titanium sulfate colorimetric assay at 300 min (a) 10 mg UMOF; (b) 30 mg UMOF; (c) 40 mg UMOF; (d) Linear correlation between absorption intensity and the corresponding concentration of H_2O_2.

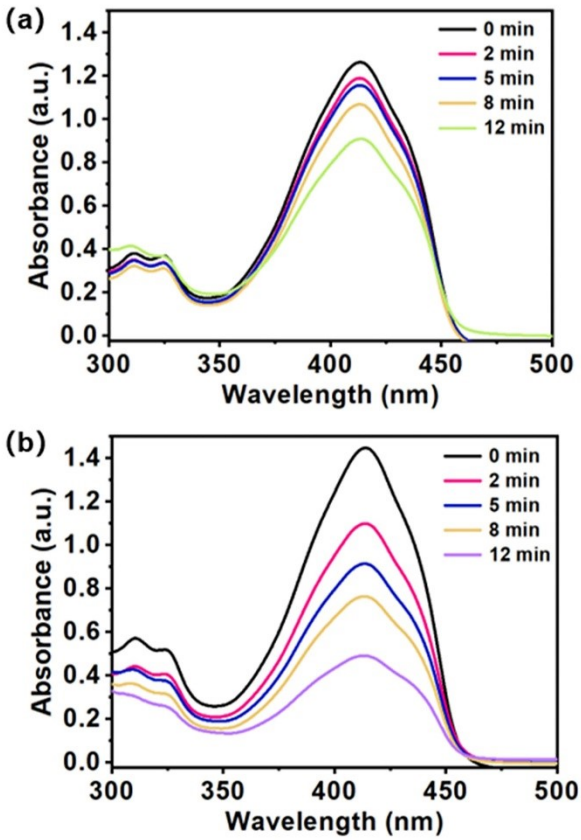

Fig. S17 UV-vis absorption spectra of DPBF in (a) H_2O_2 and (b) IMF solution upon irradiation

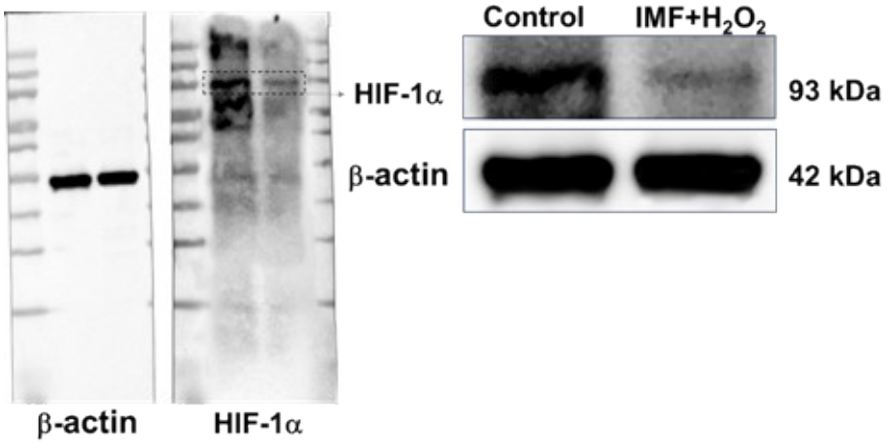

Fig. S18 The expression of HIF-1α in Hela cells with IMF+H_2O_2 treatment determined by Western blot (Protein Marker: 8-180KD).

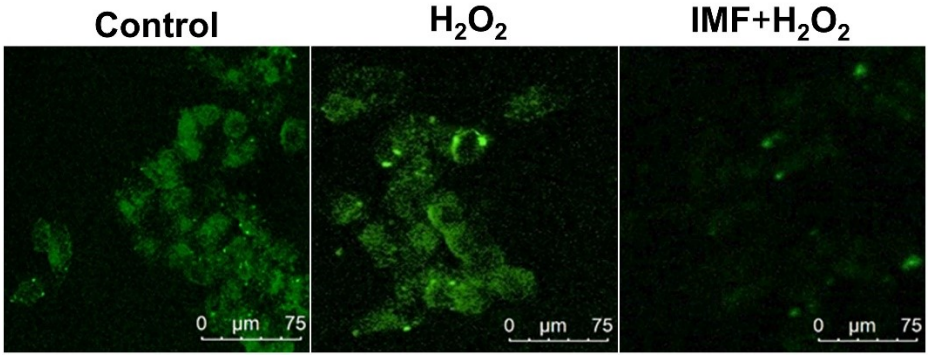

Fig. S19 Confocal images of RDPP-stained Hela cells with different treatments under hypoxia conditions. The excitation wavelength was 488 nm and the emission was collected between 500-800 nm.

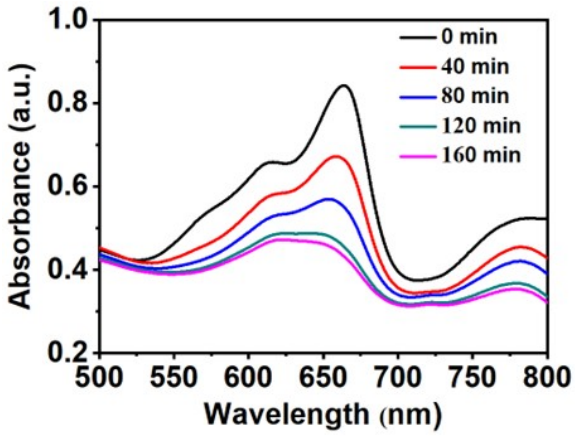

Fig. S20 UV-vis absorption spectra of MB in the presence of IMF

This oxygen generation process based on the Fe^{3+}/Fe^{2+} catalytic cycle always accompanied by ·OH generation. Methylene blue (MB) was then employed to verify the generation of ·OH. The reaction between MB and ·OH would induce a decrease in the absorption intensity of the MB. As can be seen from Fig. S14, the absorption intensity of MB at 664 nm decreased in the presence of IMF, but did not disappear completely within 160 minutes, which indicated the limited formation of ·OH along with the generation of O_2.

$Fe^{3+} + H_2O_2 \rightarrow Fe^{2+} + O_2 + H^+$

$Fe^{2+} + H_2O_2 \rightarrow Fe^{3+} + \cdot OH + OH^-$

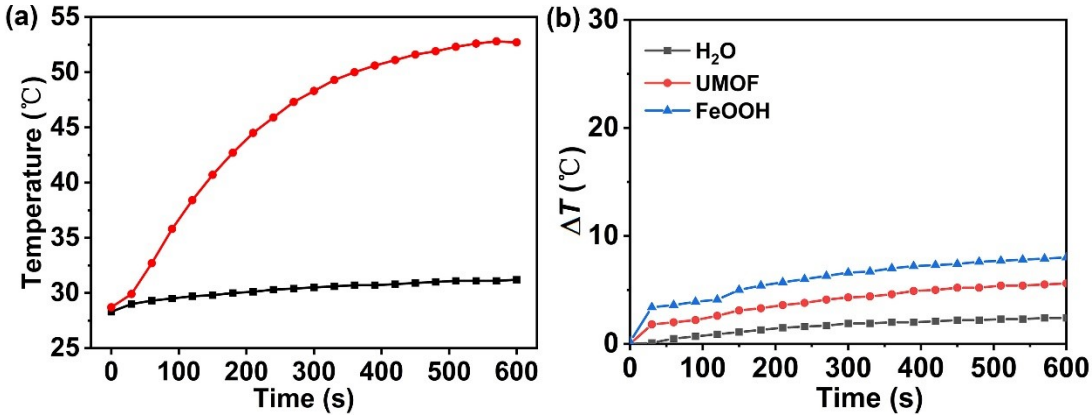

Fig. S21 (a) Temperature curves of blank control (black) and IMF (200 μg mL^{-1}) (red) with an 808 nm laser irradiation (1.5 W cm^{-2}). (b) Temperature curves of blank control and UMOF (200 μg mL^{-1}) and FeOOH (200 μg mL^{-1}) with an 808 nm laser irradiation (1.5 W cm^{-2}).

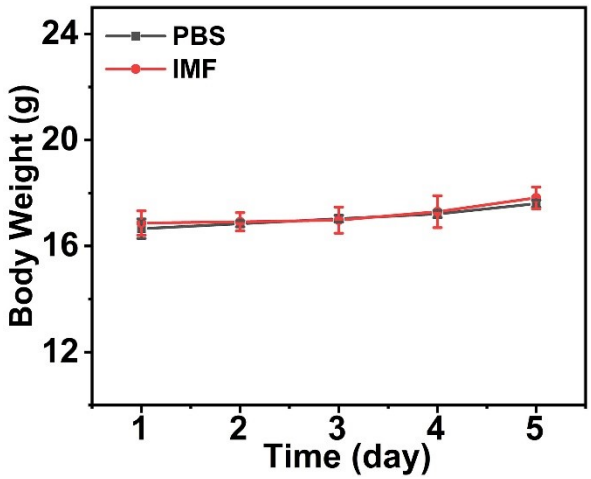

Fig. S22 Body weight curves of the normal mice with intravenous injection of PBS only and IMF only within 5 days.

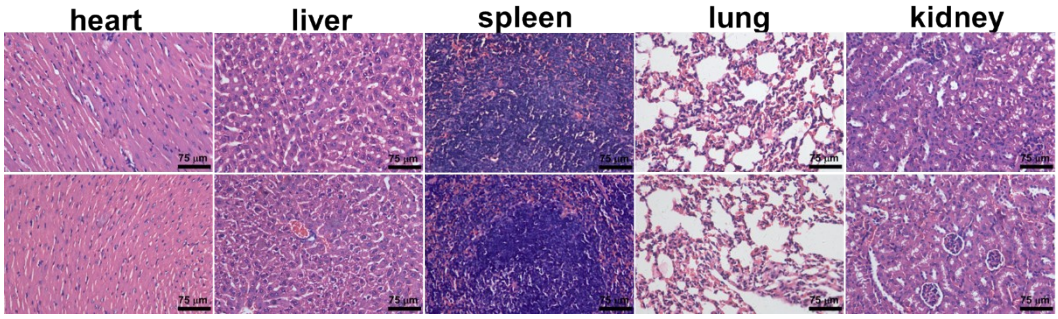

Fig. S23 H&E stained images of tissue sections from different organs of normal mice 5 days after injection of PBS only (up) and IMF only (below).

References

[1] Zhang X, Hu Q, Xia TF, Zhang J, Yang Y, Cui YJ, Chen BL, Qian GD. *ACS Appl Mater Interfaces*, 2016, 8: 32259-32265.